Mesoporous Carbon Nanospheres Featured Fluorescent Aptasensor for Multiple Diagnosis of Cancer *in vitro* and *in vivo*

Chengyi Li, Ying Meng, Shanshan Wang, Min Qian, Jianxin Wang, Weiyue Lu and Rongqin Huang*

Department of Pharmaceutics, School of Pharmacy, Key Laboratory of Smart Drug Delivery, Ministry of Education, Fudan University, Shanghai 201203, P.R. China

*Corresponding author:

Prof. Rongqin Huang, Department of Pharmaceutics, School of Pharmacy, Fudan University, 826 Zhangheng Road, Shanghai 201203, P.R. China.

Tel: +86-21-51980078

Email: rqhuang@fudan.edu.cn

Table of contents in Supporting Information:

1. **Table S1**. The performances of the OMCN/P0-Cy3 aptasensor for detecting MUC1 or MCF-7 cells in different mediums.

2. **Figure S1**. IR and Raman spectra of MCN and OMCN.

3. **Figure S2**. Quenching and recovering efficiency of OMCN/P_0-Cy3 as a function of time and concentration of OMCN, respectively.

4. **Figure S3**. Fluorescent spectra of OMCN/P_0-Cy3 in the presence of MUC1 or cells in different buffer solution, respectively.

5. **Figure S4**. Calibration curves for MUC1 detection in different buffer solution using Infinite M1000 Pro microplate reader, respectively.

6. **Figure S5.** The repeatability fluorescent spectra of OMCN/P_0-Cy3.

7. **Figure S6.** The stability fluorescent spectra of OMCN/P_0-Cy3.

8. **Figure S7.** Anti-interfering experiments of OMCN/P_0-Cy3 aptasensor.

9. **Figure S8**. The cell viability of MCF-7 and MCF-10A cells against different concentration of OMCN.

10. **Figure S9.** The confocal experiments of MCF-10A cells.

11. **Figure S10.** The inverted fluorescent imaging of kidney and liver sections.

12. **Figure S11.** *In vivo* fluorescent imaging of nude mice treated with P_0-Cy3 *via* intravenous injection.

Table S1.

The performances of the OMCN/P_0-Cy3 aptasensor for detecting MUC1 or MCF-7 cells in different mediums.

Medium	Recovery (%)			Stability[a] (%) (12 h)	Repeatability[b] (%)	
	Low (1.06 μM)	Middle (5.03 μM)	High (10.6 μM)		FS	MR
Tris-HCl	92.73	95.63	105.18	93.4	4.45	1.65
Serum	90.22	93.81	97.58	95.74	2.44	1.47
Cell	108.85	92.15	96.75	92.72	5.05	2.68

[a] The stability of OMCN/P_0-Cy3 aptasensor after storing for 12 h. [b] The RSD of five times measurements (n = 5). FS: the results of **f**luorescence **s**pectrophotometer. MR: the results of **m**icroplate **r**eader.

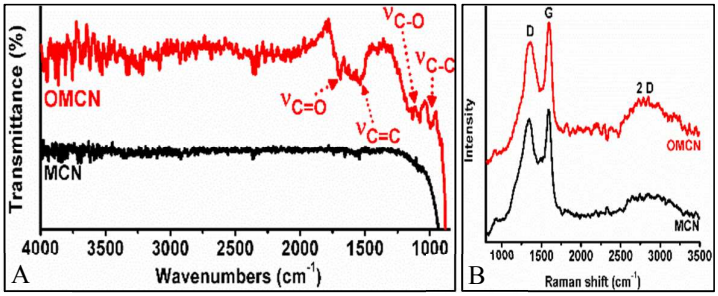

Figure S1. (A) The IR spectra of MCN and OMCN. (B) The Raman spectra of MCN and OMCN.

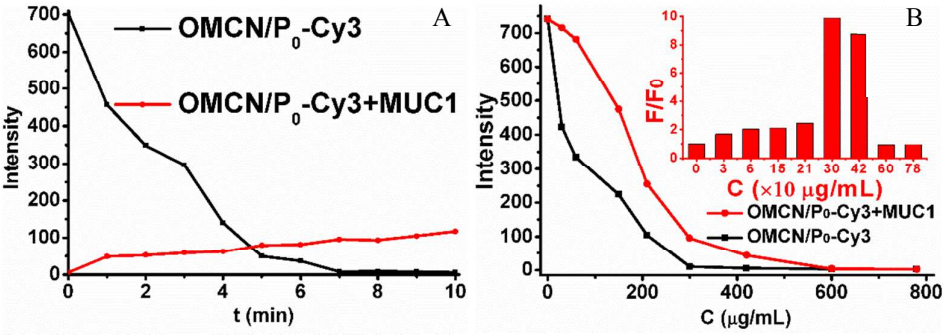

Figure S2. (A) Fluorescence quenching and recovering of the OMCN/P0-Cy3 aptasensor incubated without (black line) and with (red line) MUC1 as a function of time. (B) Effect of OMCN concentrations on the fluorescence intensity of the OMCN/P0-Cy3 aptasensor in the absence (black line) and presence (red line) of MUC1. The inset was the ratio of F/F0 as a function of OMCN concentrations. F and F0 are the fluorescence intensities with and without MUC1, respectively.

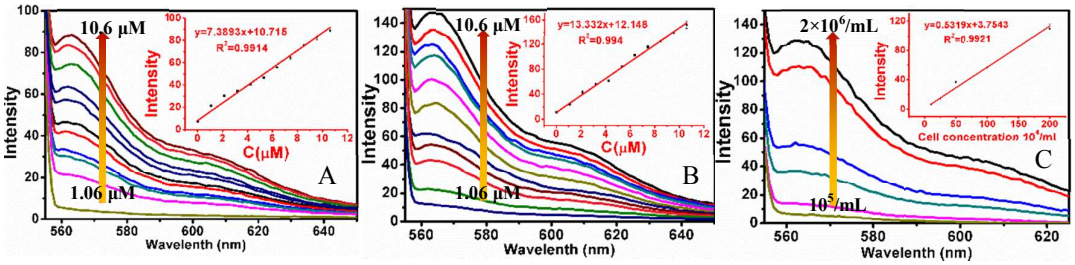

Figure S3. (A, B) Fluorescent spectra of OMCN/P_0-Cy3 in the presence of MUC1 with different concentrations in Tris-HCl solution and in 4% serum-containing buffer solution, respectively. The insets were their calibration curves for MUC1 detections. (C) Fluorescent spectra of OMCN/P_0-Cy3 in the presence of MCF-7 cells with different concentrations in Hank's buffer solution. The inset was the calibration curve for MCF-7 detection.

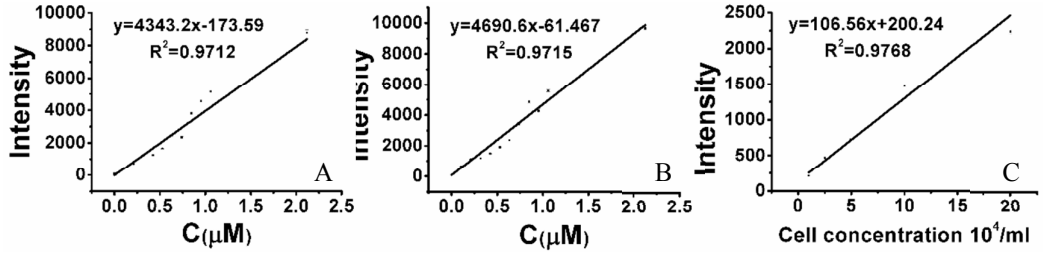

Figure S4. (A, B) The calibration curves for MUC1 detections in Tris-HCl solution and 4% serum-containing buffer solution, respectively, using the Infinite M1000 Pro microplate reader. (C) The calibration curve for MCF-7 detection in Hank's buffer solution using the Infinite M1000 Pro microplate reader.

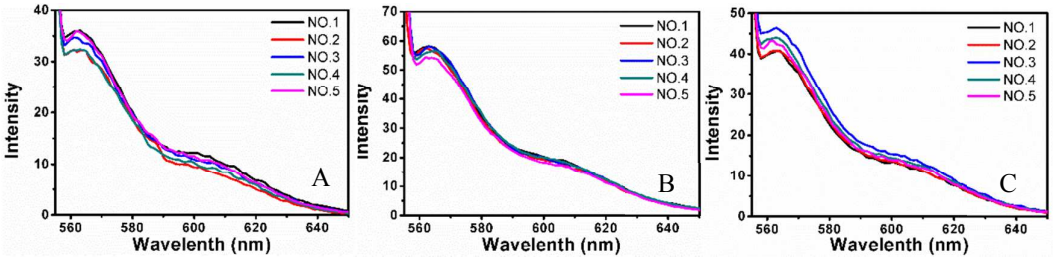

Figure S5. (A-C) Fluorescent spectra of OMCN/P_0-Cy3 upon detecting MUC1 (3.18 μM) in Tris-HCl solution (A), 4% serum-containing buffer solution (B), and 2 × 10^5 cells/mL MCF-7 cells in Hank's buffer solution (C) for 5 times, respectively.

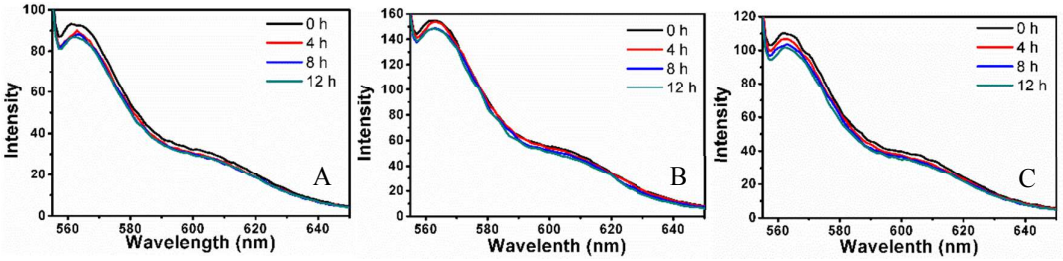

Figure S6. (A-C) Fluorescent spectra of the 0-12 h stored OMCN/P_0-Cy3 aptersensor for detecting MUC1 (10 μM) in Tris-HCl solution (A), 4% serum-containing buffer solution (B), and MCF-7 cells (2×10^6 cells/mL) in Hank's buffer solution (C), respectively.

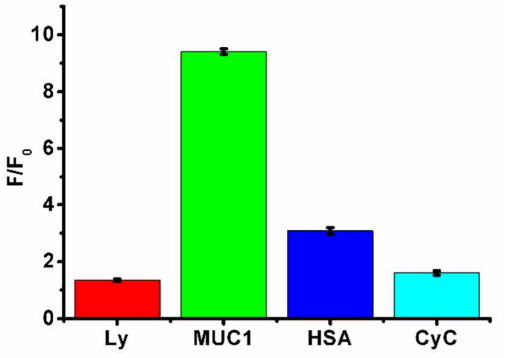

Figure S7. The F/F_0 ratios of the OMCN/P_0-Cy3 aptasensor in the presence of lysozyme (20 μM), MUC1 (10 μM), HSA (20 μM), and cytochrome C (20 μM), respectively. F and F_0 are the fluorescence intensities with and without the corresponding proteins, respectively.

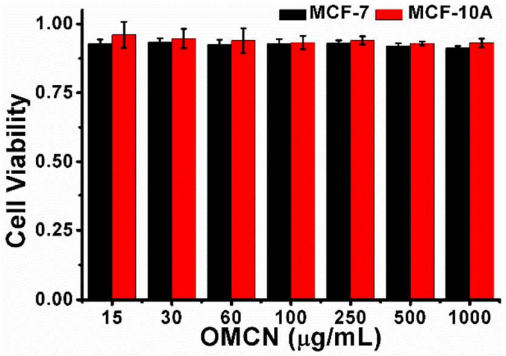

Figure S8. The viability of MCF-7 and MCF-10A cells after treating with different concentrations of OMCN for 24 h, respectively.

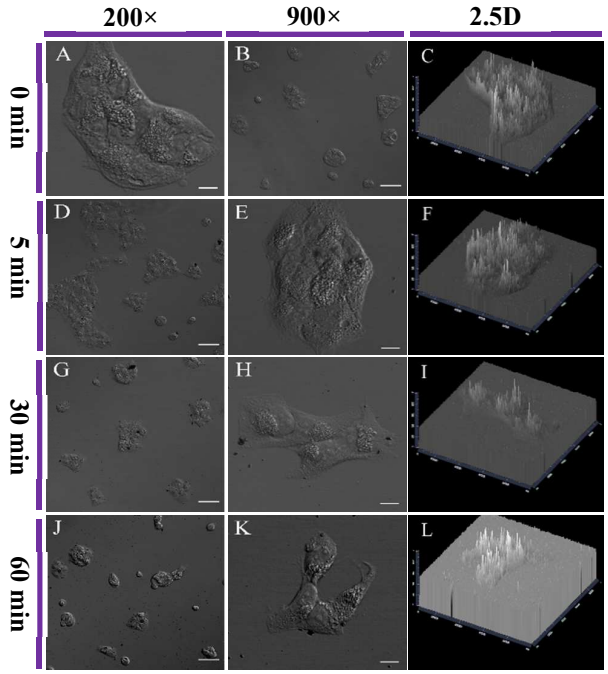

Figure S9. Different magnified confocal fluorescence microscopy images and corresponding 2.5 dimensional sectional views of MCF-10A cells incubated with OMCN/P_0-Cy3 for different time periods. Scale bar: 50 μm (200 × images), 10 μm (900 × images).

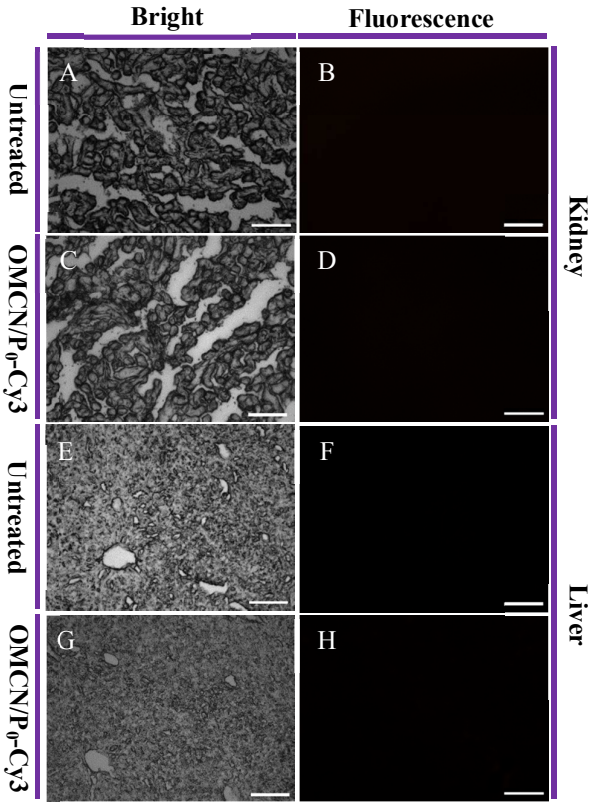

Figure S10. The inverted fluorescence microscopy images of liver and kidney sections treated without or with OMCN/P_0-Cy3. Bar = 200 μm.

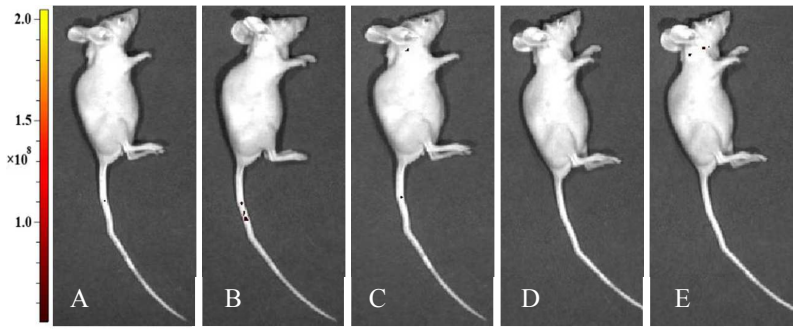

Figure S11. *In vivo* fluorescent images of normal nude mice treated with P_0-Cy3 *via* intravenous injection. Images were taken at 0 min (A), 5 min (B), 15 min (C), 30 min (D) and 60 min (E), respectively.